Implementation of Automated Cervical Cell Segmentation with Super-Pixel Partitioning and Cell-Wise Contour Refinement

Sandhu, Sukhdip
Department of Software Engineering
University of Victoria
sukhdips@uvic.ca

Cheng, David
Department of Electrical and Computer Engineering
University of Victoria
chengdavid2@gmail.com

***Abstract*—Accurate segmentation of cervical cells in microscopic images is important for the diagnosis of cervical cancer. In particular, the nucleus and cytoplasm of each cell must be detected and accurately segmented. Utilizing computer-aided diagnosis systems to automate cell segmentation is difficult due to the cell overlap and poor contrast of the cytoplasm boundaries seen in the microscopic image. H. Lee and J. Kim [1] propose a three-step automated cell segmentation method based on superpixel partitioning and cell-wise contour refinement. The first step detects the cell mass through superpixels. The second step extracts the nuclei through local thresholding. The third step partitions the superpixels and refines the boundaries through cell-wise contour refinement. The method was evaluated on the dataset provided by the ISBI 2014 challenge. The results of the evaluation displayed competitive performances with state-of-the-art methods, despite taking a much simpler approach. Our paper aims to follow Dr. Lee and Dr. Kim's implementation and evaluate it on the same dataset.**

I. Introduction

Routine screening of the Pap smear test is important in the early diagnosis of cervical cancer as it is used to detect pre-cancerous and cancerous processes of the cervix [2]. Automating the analysis of individual cervical cells obtained from the Pap smear test is important as manual analysis is time consuming and error-prone, [3] however, automating the diagnosis poses challenges particularly due to the cell-overlap and inhomogeneous cytoplasm. Delineation of the overlapped regions is particularly challenging as those regions have poor contrast. In addition, the inhomogeneous characteristic of the cytoplasm results in an environment not suitable for a threshold-based segmentation scheme to extract the cytoplasm [1].

The ISBI 2014 [1] conference publicly released a dataset of images acquired from the Pap smear test and proposed a challenge based on cell detection and cell segmentation for the automated analysis of cervical cytology specimens. The dataset consisted of both real and synthetic Pap smear images with annotated segmentation ground truths for the synthetic images. On this public dataset, recent advances in images processing have achieved state-of-the-art performances that effectively delineated the nucleus and cytoplasm of single isolated cells [3, 8, 9]. This paper evaluates a simple automatic segmentation method focusing on super-pixel partitioning and cell-wise contour refinement [1]. This method of segmentation incorporates three stages: cell mass detection, nuclei extraction and cytoplasm segmentation. The cell mass detection stage determines the initial area of interest. The nuclei extraction stage defines the placement of the cells. Lastly, the cytoplasm stage utilizes superpixel partitioning and cell-wise contour refinement to segment the cell boundaries. Dr. Lee and Dr. Kim's quantitative results of the segmentation were found to be competitive when evaluated against the state-of-the-art methods, and our implementation produces comparable results.

II. Related Work

This three stage method of utilizing superpixel partitioning and cell-wise contour refinement for the purposes of computer-aided segmentation was proposed by Lee and Kim [1] who achieved competitive results when compared to the state-of-the art methods. As for work we used, Achanta et al. [4], introduced a simple linear iterative clustering (SLIC) superpixel algorithm based on a k-means clustering technique to generate superpixels. This new algorithm outperforms existing superpixel methods in the aspect of boundary segmentation and was used as a preprocessing step in the cell mass detection and cytoplasm segmentation stages. In G. W. Zack et al. [5], the triangle thresholding algorithm was introduced and was used to select the threshold in the cell mass detection stage. This thresholding technique effectively detects the cell mass where variations in the intensity due to overlapping cell create difficulties in obtaining the optimal threshold. In Phansalkar et al. [6], the adaptive local thresholding scheme was introduced which proposed to address the problem of non-homogenous staining of the cell due to low contrast dark regions corresponding to the nuclei. This local thresholding scheme performed better than the commonly used Otsu's method and Sauvola's method in the cytology image analysis environment and was used in the nuclei extraction stage. In Rother et al. [7], a simplified iterative graph-cut approach to segmentation of foreground and background achieved high performance at the cost of modest user interactive. This algorithm was implemented as a built-in MATLAB function and was used in the cell-contour refinement step in the final cytoplasm segmentation.

The results of this implementation were compared to the results of the originator, Lee and Kim [1], in addition to 3 state-of-the-art cervical cell segmentation methods [3, 8, 9]. In Lu et al. [3], a segmentation approach was used that was

[1] https://cs.adelaide.edu.au/~carneiro/isbi14_challenge/index.html

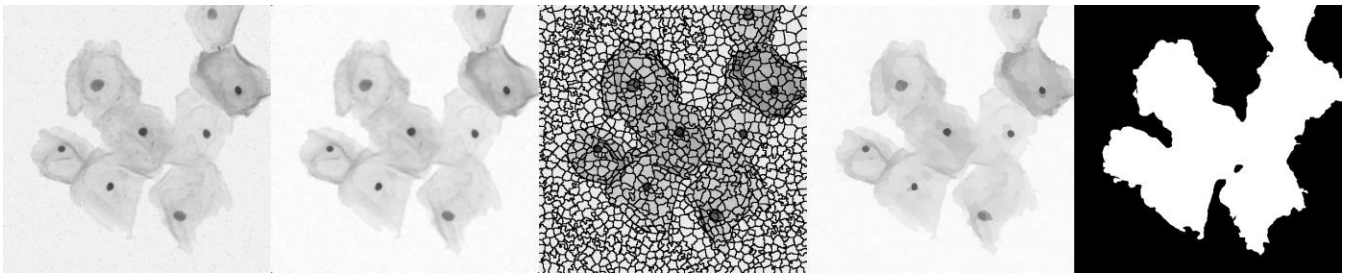

(a) Input image (b) Pre-processed image (c) Superpixel image (d) Mean image (e) Detected cell mass

Figure 1: Cell Mass Detection: (a) original image, (b) pre-processed image, (c) superpixel over segmentation, (d) mean image, (e) cell mass

based on the joint optimization of multiple level set functions [10] where each function represents a cell within a clump that have both unary and pairwise constraints. In Ushizima et al. [8], a segmentation approach was used that was based on cellular mass estimation by superpixel clustering and triangle algorithm, nuclei detection and cytoplasm detection through graph-based region growing and Voronoi Diagrams was used. In Nosrati et al. [9], a segmentation approach was used that was based off extracting the cell nuclei by utilizing both a maximally stable extremal region detector (MSER) [11] and a random forest classifier. Corresponding cytoplasm was then represented as multiple signed distance functions and the boundaries refined further by Chan-Vese method [12]

III. Proposed Approach

The methods are divided into three main components: cell mass detection, nucleus extraction, and cytoplasm segmentation. Each of these main components are further subdivided into methods, see Fig. 2. Note, the algorithm is linear in nature, with each subsequent method relying on the output of the previous step. The following section will outline each method, as well as any deviations/improvements from the original paper we made.

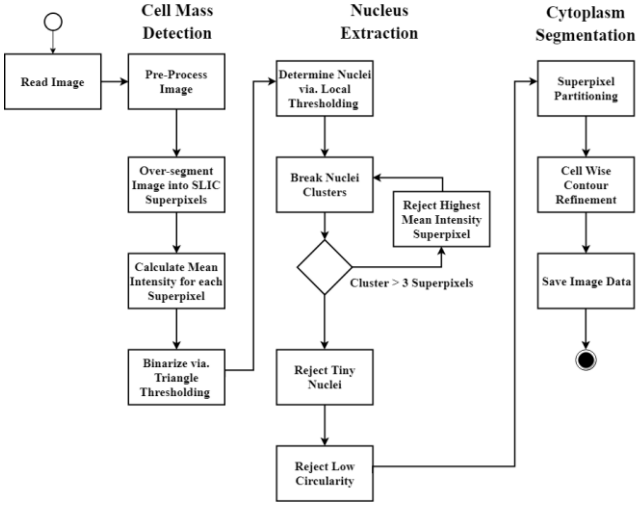

Figure 2: Block diagram form of algorithm design

A. Cell Mass Detection

The objective of cell mass detection is to segment the image into two regions, everything that is part of the cell (referred to as cell mass), and everything that is not. This segmented cell mass is thereby used as the region of interest moving forward. Firstly, a 2-D median filter is applied over the entire image to reduce noise. A 5x5 neighbourhood kernel size is used as we found this yielded the best results. Afterwards, we added an additional preprocessing step of normalizing the image to range [0,1] with the intention to speed up following computations, and further increase cell to background contrast as shown in Fig. 1 (b). Next, the image is oversegmented into superpixels by the SLIC method [4], Fig. 1 (c). The number of superpixels to create was treated as a hyperparameter as the paper did not specify. The optimal value we determined was to create *3 times the image width* number of superpixels. For the 512x512 image, this meant breaking into 1536 superpixels. This effectively reduces the search space from the original 262,144 pixels to 1536 superpixels. For each of these superpixels, the mean intensity values are computed to generate the mean-value image Fig. 1 (d). From this mean-value image, the cell mass, Fig. 1 (e) is extracted using the adaptive triangle thresholding method [5]. The algorithm defines the threshold as the location where the distance of a curve through the histogram from a line through the two maxima is maximum. The outcome of the triangle thresholding technique results in many false positive superpixels being classified as part of the cell mass, so we opted to add an additional morphological open operation to remove small objects from the binary image.

The extraction cell mass is used as the search area for nucleus segmentation and cytoplasm segmentation

B. Nucleus Extraction

The aim for the nucleus extraction methods are to extract the nuclei of cells to locate individual cells in the cell mass. This operates under the fundamental assumption that each individual cell has only one nucleus. A local thresholding technique designed by Phansalkar et al. [6] specifically for low contrast cytology images is used to extract nuclei since the nuclei are usually darker than their surrounding cytoplasm.

In local thresholding, the threshold T for each superpixel is determined as

$$T = \mu(1 + p * \exp(-q\mu) + k(\sigma/s - 1)) \qquad (1)$$

where μ, σ are mean and standard deviation of local window intensities, respectively, and $p = 2$, $q = 10$, $k = 0.25$, $s = 1$ are weighting variables. The local window for each superpixel is defined as a group of superpixels whose distances between the centers are less than $d = 0.1 \times l$ where l is image width. Then, superpixels with mean intensities less than the locally defined threshold T are classified as initial nucleus candidates. While this method performs well, it also extracts non-nucleus outliers, see Fig. 3 (b), thus, three methods are further performed to refine the extracted nuclei: breaking superpixel clusters, rejecting tiny superpixels, and rejecting nucleus candidates with low circularity.

(a) (b) (c)

Figure 3: Nuclei extraction; (a) original image, (b) initial nuclei candidates, (c) nuclei candidates after outlier removal

Firstly, clustered superpixels, defined as containing more than three superpixels can be considered to have an outlier candidate in it. These clustered regions are determined by connected component labeling, and for each cluster containing more than three superpixels, the superpixels with the highest intensity are iteratively removed.

Second, rejecting tiny superpixel method rejects those nuclei candidate superpixels with an area less than 30 pixels.

Lastly, candidates with low circularity, ρ, as determined by

$$\rho = 4\pi \frac{A}{P^2} \qquad (2)$$

where A, P are the area and the perimeter of a candidate region, respectively, are removed. For reference, (2) for a perfect circle yields $\rho = 1.0$, and for a perfect square yields $\rho = 0.785$. The paper specifies that those with $\rho < 0.5$ are removed, however after parameter tuning our findings show that $\rho < 0.675$ yields better results.

After the refinement methods, the refined nuclei candidates are extracted, see Fig. 3 (c). These nuclei are used as indicators in cytoplasm segmentation.

C. Cytoplasm Segmentation

In cytoplasm segmentation, the boundaries of individual cytoplasm are determined by superpixel partitioning and cell-wise contour refinement. Initially, superpixel partitioning determines boundaries by labelling non-nucleus superpixels as part of the cell with the nearest nucleus as determined by Euclidean distance. This provide an adequate approximation of individual cell boundaries but suffer from noisy boundaries and the inability to deal with overlapping regions. Figure 4 illustrates segmentation performed by superpixel partitioning, note that by the nature of the algorithm, a superpixel cannot be classified as being part of more than one cell, so overlapping regions are completely void. Moreover, the boundaries are jagged, often times with sharp corners which is unlike the topology of cells. Cell-wise contour refinement

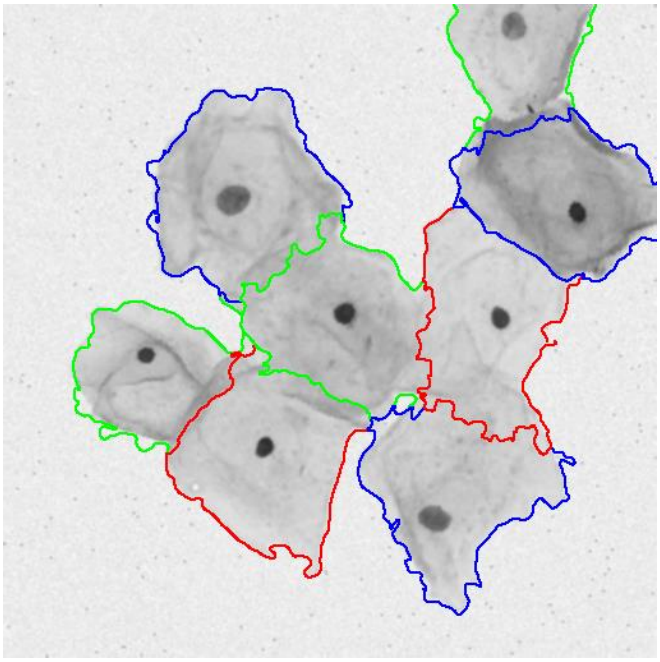

Figure 4: Superpixel partitioning segmentation

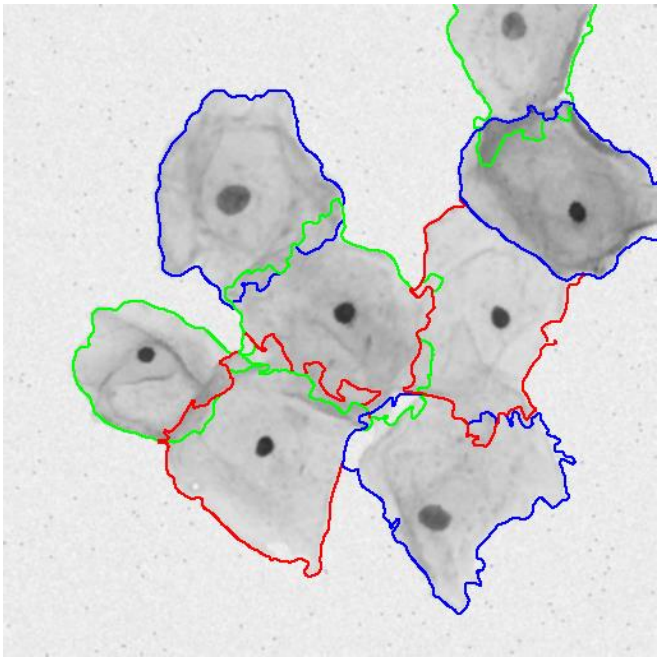

Figure 5: Cell-wise contour refinement segmentation

aims to solve these problems.

Boundaries are further refined via cell-wise contouring, seen in Fig. 5. The paper uses a Graph Cut [13] segmentation algorithm however we opted to use GrabCut [7] – an alternative graph segmentation algorithm based off Graph Cuts – as it is part of MATLABs Image Processing Toolbox. The parameters to specify for GrabCut are the foreground and background masks, i.e. regions that specify pixels in the image that foreground and background respectively. These regions are defined by morphological operations, were the foreground is the erosion of the initial segmentation performed by superpixel partitioning, and the background is the dilation.

IV. Evaluation Results

A. Description of Database

The dataset was obtained from the Overlapping Cytology Image Segmentation Challenge held in ISBI 2014 and consisted of 16 Extended Depth of Field (EDF) real cervical cytology images and 900 synthetic images. The qualitative assessment was performed on the 16 EDF real cervical cytology images and the quantitative evaluation was performed over all 900 synthetic images. This decision was made as the ground truth cytoplasm segmentation was not available for the real EDF images.

B. Algorithm Metrics

Using non-optimized MATLAB code on an Intel® Core™ i7-4720HQ CPU @2.60 GHz with 16 GB RAM, our segmentations perform in ~4.6 seconds per (512x512) synthetic image, and ~2.5 minutes per (1024x1024) real image.

C. Evaluation Metrics

To validate our methods, quantitative measurements [2] including, Dice coefficient (DC), object-based false negative (FN_O), pixel-based true positive (TP_P), and pixel-based false positive (FP_P) between our segmentation and the ground truth data were determined. (3)

$$DC = \frac{2|A \cap B|}{|A| + |B|} \tag{4}$$

$$FN_o = \frac{DC \leq 0.7}{N_{Total}} \tag{5}$$

$$TP_P = \frac{N_{TP}}{N_{TP} + N_{FN}} \tag{6}$$

$$FP_P = \frac{N_{FP}}{N_{FP} + N_{TN}}$$

To evaluate the implementation quantitatively, the DC as seen in (3) of the final segmentation is computed against the provided ground truth annotations . This coefficient measures the similarity between the algorithm's boundary output and the ground truth. If the two segmentations are identical, the coefficient is equal to 1.0, while if the segmentation and ground truth have no elements in common, the coefficient is equal to 0.0. A DC greater than 0.7 is considered a good segmentation. The average DC value for the segmentations that were considered good were was computed.

The success rate of our implementation is calculated as the FN_O as seen in (4). The FN_O was computed as a ratio of cells with DC $\leq$ 0.7 to the total number of segmentations. This allows us to evaluate the percentage of good segmentations that our algorithm produces.

The quality of our successful segmentations was calculated as the average values of the DC, TP_P and FP_P for the segmentations with DC > 0.7. The TP_P rates are calculated as seen in (5) and represent the pixels correctly segmented as foreground where N_{TP} and N_{FN} are the number of pixels identified as true positives and false negatives respectively. The FP_P rates are calculated as seen in (4) and represent pixels falsely segmented as foreground where N_{FP} and N_{TN} are the pixels identified as false positives and true negatives. These three metrics indicate the quality of the segmentations that were considered good. *Table 1 references these metrics for convenience.*

TABLE I
Evaluation Metric Reference

Symbol	Definition
DC	Dice Coefficient
FN_O	Object-Based False Negative
TP_P	Pixel-Based True Positive
FP_P	Pixel-Based False Positive
N_{TP}	Number of Pixel True Positive
N_{FN}	Number of Pixel False Negatives
N_{FP}	Number of Pixel False Positive
N_{TN}	Number of Pixel True Negative
N_{TOTAL}	Total Number of Segmentations

These metrics were chosen in particular to allow for consistent evaluation to state-of-the-art Pap Smear segmentations methods [1, 3, 8, 9].

D. Quantitative Evaluation Results

The results of evaluating the algorithm over the provided 900 synthetic test images are summarized in Table 2 in addition with the results provided for those of state-of-art methods. The average of the state-of-the-art methods are also calculated to provide measure of expectancy. Over the good segmentations, the algorithm saw a comparable DC value of 0.867, TP_P of 0.837 and FP_P of 0.002. The FN_O saw a value of 0.245.

The standard percent error was calculated between our results to the result of Lee and Kim [1], and to the mean of the four state-of-the-art methods. The results were within range of the accepted methods with a DC percent error of 3.31%, a TP_P percent error of 5.07% , a FP_P percent error of 0% , and a FN_O percent error of 78.54%, when compared to Lee and Kim [1] whose methodology we followed for segmentation.

Table 2: Evaluation and comparison of our implementations segmentation results vs. the papers and other state-of-the-art methods

METHODS	DC	FN_O	TP_P	FP_P
OUR APPROACH	**0.867 ± 0.078**	**0.242 ± 0.270**	**0.838 ± 0.116**	**0.002 ± 0.003**
LEE AND KIM [1]	0.897 ± 0.075	0.137 ± 0.194	0.882 ± 0.097	0.002 ± 0.002
USHIZIMA ET AL. [8]	0.872 ± 0.082	0.267 ± 0.278	0.841 ± 0.130	0.002 ± 0.003
NOSRATI ET AL. [9]	0.871 ± 0.075	0.111 ± 0.166	0.875 ± 0.086	0.004 ± 0.004
LU ET AL. [3]	0.893 ± 0.082	0.316 ± 0.295	0.905 ± 0.096	0.002 ± 0.005
MEAN OF PUBLISHED METHODS	*0.883 ± 0.079*	*0.208 ± 0.233*	*0.876 ± 0.102*	*0.003 ± 0.004*

The FN_O percent error is high when compared to Kim and Lee, however, the FN_O showed high variance across the accepted methods with a percent error ranging from 8.39% with Ushizima et al. [8] to 120.36% with Nosrati et al. [9]. When compared to mean of the published methods, results, the DC has a percent error of 1.81%, the TP_P percent error of 4.39% , a FP_P has a percent error of 22.86% , and a FN_O percent error of 17.74%. Compared to Lee and Kim, our results are similar, though noticeably underperforms in all evaluated fields, but when compared to the mean of the published methods, our results are competitive.

E. Qualitative Evaluation Results

The qualitative evaluation was preformed on the 16 real EDF microscopy images of cervical cells to get a real-world representation of the results. Analyzing the cytoplasm segmentation stage, the integration of the graph segmentation algorithm showed strength in segmenting outer boundaries of the cell. In Fig. 6 (a) it can be seen that the initial superpixel partitioning developed outer boundaries that included sharp peaks and outliers. However, after applying cell-wise contouring using the graph-based method, the outer boundaries showed improvements to the delineation along the cell and that outliers were removed. This improvement in segmentation can be seen clearly in Fig. 6 (b) where the outer edges of the boundaries have contracted closer to the actual cell and the majority of the outliers have been removed. Furthermore, although minimal, some boundaries do begin to segment overlapping regions.

V. DISCUSSION

The resulting FN_O was found to be high and can be attributed to the nuclei extraction stage of the algorithm. The algorithm saw over segmented nucleus regions as it is designed to detect them via an adaptive thresholding technique based off intensity change from its surrounding. In general, this algorithm works well, but in areas where there is significant intensity difference, as seen in Fig. 7 (a) near the bottom of the rightmost cell, a false detection of a nucleus is detected. As the nuclei location is used to map the superpixels to the corresponding cytoplasm, the segmentation attempt without accurate nuclei detection results in a poor segmentation. This goes on to negatively contribute to the FN_O rate as this cell segmentation, as well as its neighbouring cells DC value compared to the ground truth are likely ≤ 0.7 and classified as poor.

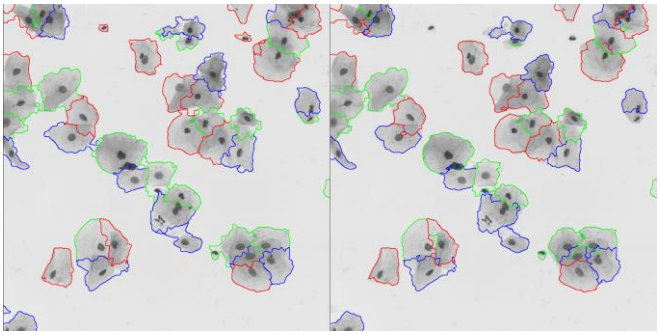

(a) Superpixel partitioning (b) Cell-wise contour refinement

Figure 6: Qualitative evaluation (a) superpixel partitioning, (b) cell-wise contour refinement

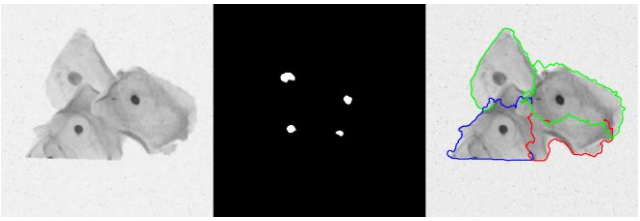

(a) (b) (c)

Figure 7: (a) Original image and its resulting (b) false nuclei detection and (c) segmentation

VI. Conclusion

In summary, following the Lee and Kim algorithm to solving the complex segmentation of cervical cytology images has proven successful. Our results are comparable to their results, and well within the expected range of error. As well, when compared to the other state-of-the-art methods, our method offers competitive results, in some cases even generating better results. Figures 8 through 11 illustrate in graphical form the results of Table 2.

Lee and Kim acknowledge that further work is to be done on the nucleus detection method. When qualitatively analyzing images, its clear that for most images, the nuclei are either over segmented or under segmented by 1-2 nuclei. Should these be corrected, we expect the algorithm to yield significantly improved results. In addition, more parameter tuning can be tested to achieve higher results. In our case, we parameter tuned on the provided training subset of 45 images due to the significantly lower run time (4.5 minutes/45 images vs. 70 minutes/900 images). Most notably, the FN_O rate on the training dataset is 19.63% which is very good, and what we aim to improve on the testing dataset. Lastly, future work can be done to implement the Graph Cut [13] algorithm used in the paper. That said, utilizing the simpler GrabCut algorithm [7], we were able to achieve excellent performance, while further simplifying the simple approach Dr. Lee and Dr. Kim proposed.

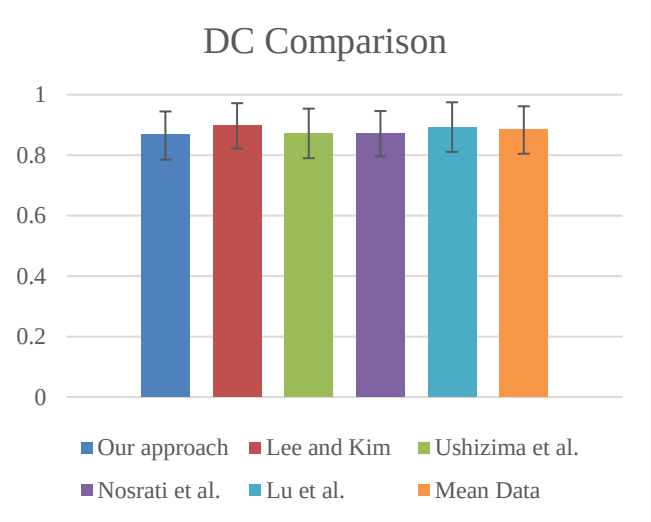

Figure 8: Comparing DC results

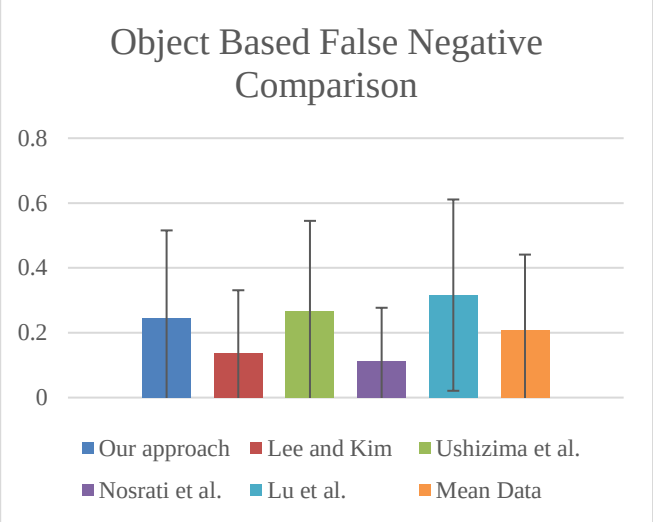

Figure 9: Comparing FN_O results

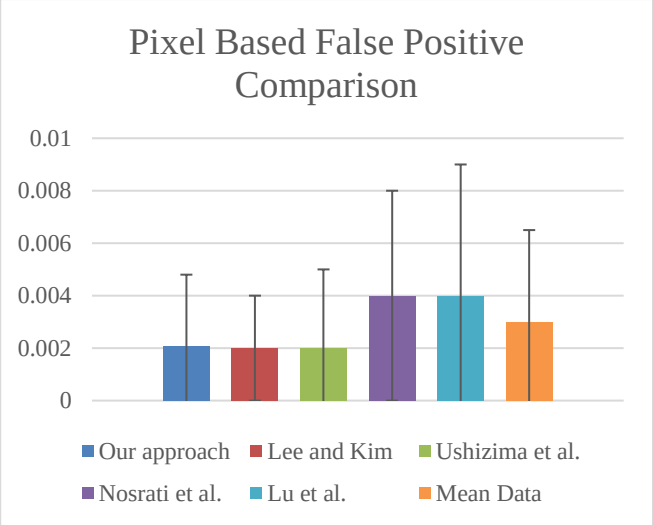

Figure 10: Comparing FP_P results

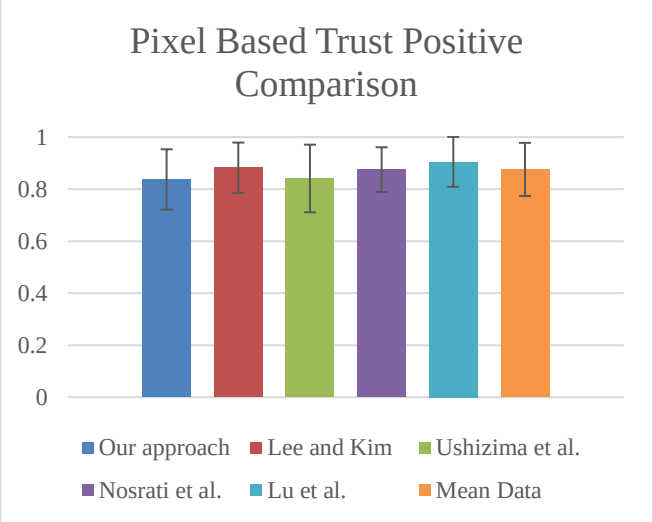

Figure 11: Comparing TP_P results

ACKNOWLEDGMENT

First and foremost, we like to acknowledge Dr. Alexandra Branzan Albu, our professor who has taught us various aspects of Medical Image Processing at the University of Victoria. Moreover, many thanks are due to the University of Victoria for allowing us access to various published research online. Lastly, we would like to acknowledge the hosts of the competition, as well as the numerous researchers who's work, we've based our solutions around. And of course, special thanks to Dr. Lee and Dr. Kim for provided the analysis method we based our implementation around.

REFERENCES

[1] H. Lee and J. Kim, "Segmentation of Overlapping Cervical Cells in Microscopic Images with Superpixel Partitioning and Cell-Wise Contour Refinement," 2016 *IEEE Conference on Computer Vision and Pattern Recognition Workshops* (CVPRW), Las Vegas, NV, 2016, pp. 1367-1373. doi: 10.1109/CVPRW.2016.172

[2] Z. Lu, G. Carneiro, and A. Bradley. An improved joint optimization of multiple level set functions for the segmentation of overlapping cervical cells. *Image Processing, IEEE Transactions on*, 24(4):1261–1272, April 2015.

[3] Z. Lu, G. Carneiro, A. Bradley, D. Ushizima, M. S. Nosrati, A. Bianchi, C. Carneiro, and G. Hamarneh. Evaluation of three algorithms for the segmentation of overlapping cervical cells. *IEEE Journal of Biomedical and Health Informatics*, PP(99):1–1, 2016.

[4] R. Achanta, A. Shaji, K. Smith, A. Lucchi, P. Fua, and S. Susstrunk. Slic superpixels compared to state-of-the-art superpixel methods. *IEEE Trans. Pattern Anal. Machine Intel.*, 34(11):2274–2282, Nov 2012.

[5] G. Zack, W. Rogers and S. Latt, "Automatic measurement of sister chromatid exchange frequency.", *Journal of Histochemistry & Cytochemistry*, vol. 25, no. 7, pp. 741-753, 1977. Available: 10.1177/25.7.70454.

[6] N. Phansalkar, M. Sangram and S. Anima, "Adaptive local thresholding for detection of nuclei in diversity stained cytology images", *2011 International Conference on Communications and Signal Processing (2011): 218-220*, 2011. [Accessed 11 April 2019].

[7] C. Rother, V. Kolmogorov and A. Blake, ""GrabCut"", *ACM Transactions on Graphics*, vol. 23, no. 3, p. 309, 2004. Available: 10.1145/1015706.1015720.

[8] D. M. Ushizima, A. G. C. Bianchi, and C. M. Carneiro. Segmentation of subcellular compartments combining superpixel representation with voronoi diagrams. In *Overlapping Cervical Cytology Image Segmentation Challenge - ISBI 2014*, 2014.

[9] M. S. Nosrati and G. Hamarneh. A variational approach for overlapping cell segmentation. *In Overlapping Cervical Cytology Image Segmentation Challenge - ISBI 2014*, 2014.

[10] M. Rousson and N. Paragios. Computer Vision — *ECCV 2002: 7th European Conference on Computer Vision* Copenhagen, Denmark, May 28–31, 2002 Proceedings, Part II, chapter Shape Priors for Level Set Representations, pages 78–92. Springer Berlin Heidelberg, Berlin, Heidelberg, 2002.

[11] J. Matas, O. Chum, M. Urban, and T. Pajdla. Robust widebaseline stereo from maximally stable extremal regions. *Image and Vision Computing*, 22(10):761 – 767, 2004.

[12] T. F. Chan and L. A. Vese. Active contours without edges. *IEEE Transactions on Image Processing*, 10(2):266–277, Feb 2001.

[13] Y. Boykov and M.-P. Jolly. Interactive graph cuts for optimal boundary amp; region segmentation of objects in n-d images. In *Proc. IEEE Intl. Conf. Computer Vision*, volume 1, pages 105–112 vol.1, 2001.